The microbiota regulates murine inflammatory responses to toxin-induced CNS demyelination but has minimal impact on remyelination

Christopher E McMurran[1], Alerie Guzman de la Fuente[1,2], Rosana Penalva[2], Ofra Ben Menachem-Zidon[1,3], Yvonne Dombrowski[2], John Falconer[2], Ginez A Gonzalez[1], Chao Zhao[1], Fynn N Krause[4], Adam MH Young[1], Julian L Griffin[4], Clare A Jones[5], Claire Hollins[5], Markus M Heimesaat[6], Denise C Fitzgerald[2*] and Robin JM Franklin[1*]

[1] Wellcome - MRC Stem Cell Institute, University of Cambridge, Cambridge, UK, CB2 0AH[2] Wellcome - Wolfson Institute for Experimental Medicine, Queen's University Belfast, Belfast, UK, BT9 7BL [3] Hadassah Human Embryonic Stem Cell Research Center, Goldyne Savad Institute of Gene Therapy, Hadassah-Hebrew University Hospital, Jerusalem, Israel, 91240 [4] Department of Biochemistry, University of Cambridge, Cambridge, UK, CB2 1GA [5] ☐Respiratory, Inflammation and Autoimmunity Research, MedImmune Ltd, Cambridge, UK, CB21 6GH [6] ☐Charité - University Medicine Berlin, Institute for Microbiology, Infectious Diseases and Immunology, 14195 Berlin, Germany * **Corresponding authors:** DCF - d.fitzgerald@qub.ac.uk, RJMF - rjf1000@cam.ac.uk

Submitted to Proceedings of the National Academy of Sciences of the United States of America

The microbiota is now recognised as a key influence on the host immune response in the central nervous system (CNS). As such, there has been some progress towards therapies that modulate the microbiota with the aim of limiting immune-mediated demyelination, as occurs in multiple sclerosis. However, remyelination – the regeneration of myelin sheaths – also depends upon an immune response, and the effects that such interventions might have on remyelination have not yet been explored. Here, we show that the inflammatory response during CNS remyelination in mice is modulated by antibiotic or probiotic treatment, as well as in germ-free mice. We also explore the effect of these changes on oligodendrocyte progenitor cell differentiation, which is inhibited by antibiotics but unaffected by our other interventions. These results reveal that high combined doses of oral antibiotics impair oligodendrocyte progenitor cell responses during remyelination and further our understanding of how mammalian regeneration relates to the microbiota.

microbiota | remyelination | microglia | macrophage | oligodendrocyte progenitor cell

Introduction

Our knowledge of the microbiota and its relationship with host immunity, metabolism and neurobiology has significantly expanded in recent years (1). However, the role of the microbiota in mammalian regeneration remains relatively unexplored. As endogenous tissue regeneration is facilitated by a local immune response (2), it is feasible that intestinal microbes, which modulate the host immune system (3, 4), could help shape the outcome of regeneration in a clinical setting. The gut microbial community can be easily modified using oral antibiotics or probiotics, thus addressing this question is of great clinical relevance.

Here, we investigate how the intestinal microbiota influences remyelination, the most effective form of regeneration observed in the mammalian central nervous system (CNS) and a promising therapeutic strategy for multiple sclerosis (MS) and other myelin diseases (5). Successful remyelination can bring functional recovery (6, 7) and protect axons from degeneration (8). This success depends on an inflammatory response by microglia and infiltrating macrophages (9) that progresses and resolves appropriately (10, 11). Due to its distance from any epithelial interface with environmental microbes, CNS remyelination is an ideal model to explore systemic influences of the microbiota on regeneration.

The rationale for our studies is based on the close relationship between remyelination and the innate immune response, and in turn between the immune system and the microbiota. To create an environment that permits remyelination, endogenous microglia and infiltrating macrophages must clear myelin debris remaining from the disintegrated sheath (12), and also secrete pro-regenerative factors (10, 11, 13). These roles hinge upon a coordinated immune response to demyelination, failure of which can impair remyelination, as occurs in older animals (14, 15). Meanwhile, there is now a substantial body of evidence linking the microbiota to CNS inflammation across various contexts. For example, germ-free or antibiotics-treated mice have transcriptionally immature microglia, which have an impaired response to lipopolysaccharide (LPS) or viral stimulation (3), whilst antibiotic depletion of the microbiota reduces monocyte entry into the brain (4). The immune system is therefore a strong candidate for conveying an influence from the microbiota to regeneration in distant tissues such as the CNS.

There is a growing appreciation of the relationship between the microbiota and MS. Patients with MS have a distinct microbiome compared to healthy controls (16, 17), and this may have a role in disease pathogenesis, given that faecal transplant from patients with MS can provoke immune-mediated demyelination in predisposed germ-free mice (18). Much focus has centred upon antibiotic or probiotic interventions that aim to limit demyelination in MS and animal models (19–21). However, the effects

Significance

People with multiple sclerosis have a distinct microbiota to healthy controls, and there is growing interest in how these differences might contribute to the onset and progression of CNS autoimmunity. However, the impact that the microbiota may also have on the endogenous regeneration of myelin – remyelination – has not yet been explored. Here we show that inflammatory responses during remyelination depend upon the microbiota, being modulated by antibiotics, probiotics or in germ-free mice. In contrast, these interventions had minimal impact on the activity of oligodendrocyte progenitor cells, with only supra-therapeutic doses of antibiotics having an inhibitory effect. Our results suggest that endogenous CNS remyelination is largely resilient to interventions that modify the microbiota.

Reserved for Publication Footnotes

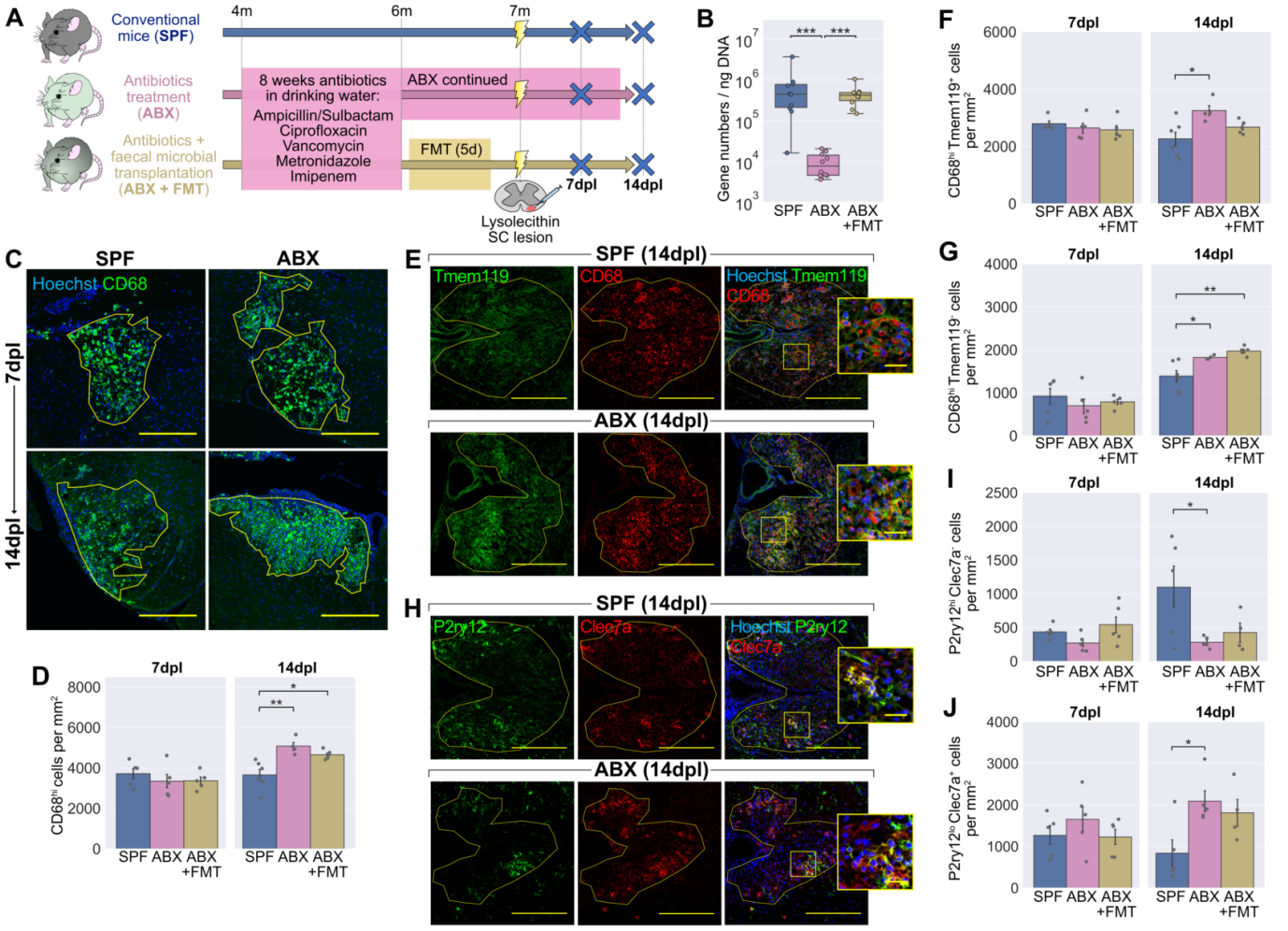

Fig. 1. **Antibiotics treatment to deplete the microbiota alters the inflammatory response following lysolecithin-mediated demyelination.** (**A**) Mice were administered ABX in their drinking water for 2 months, after which one group received a faecal microbial transplant (FMT) whilst another group were continued on ABX. Mice were sacrificed at 7 and 14 days following lysolecithin injection into the ventral white matter of the spinal cord. (**B**) RT-PCR of faecal DNA showing depletion of the microbiota by ABX and return to normal levels with FMT. (**C-D**) Representative images (**C**) and density (**D**) of $CD68^{hi}$ activated microglia/macrophages within the lesion boundary (yellow line). (**E-G**) Representative images (**E**) and density of $Tmem119^{+}CD68^{hi}$ microglia-derived (**F**) and $Tmem119^{-}CD68^{hi}$ monocyte-derived (**G**) $CD68^{hi}$ cells within lesions. (**H-J**) Representative images (**H**) and density of $P2ry12^{hi}Clec7a^{-}$ homeostatic (**I**) and $P2ry12^{lo}Clec7a^{+}$ (**J**) degeneration-associated microglia/macrophages within lesions. Scale bars: (**C**) = 250μm, (**E, H**) = 200μm [inset: 25μm]. Insets (**E, H**) are a 3x magnification of the boxed regions. Error bars show mean ± SEM; *p<0.05, **p<0.01, ***p<0.001; (**B**) Kruskal-Wallis with Dunn's *post hoc* test; (**D, F-G, I-J**) one-way ANOVA with Tukey HSD *post hoc* test, n=4-6 mice.

that such treatments might have on remyelination remain to be elucidated.

Here we use a variety of interventions to alter the murine microbiota, before quantifying inflammation and oligodendrocyte progenitor cell (OPC) activity in response to toxin-induced demyelination. Across antibiotics-treated, probiotic-treated and germ-free mice, altering the microbiota was found to modulate the inflammatory response following demyelination. However, no clear relationship emerged between the microbiota, the OPC response to demyelination and subsequent remyelination.

Results

Combined antibiotics treatment to deplete the microbiota alters inflammation following toxin-induced demyelination

To explore whether extensive microbial depletion would affect remyelination, C57BL/6 mice were administered broad-spectrum antibiotics (ABX) in their drinking water for 8 weeks (**Fig. 1A**). This combination of ampicillin/sulbactam, ciprofloxacin, vancomycin, metronidazole and imipenem has previously been shown to cause depletion of the microbiota (4), which we confirmed by quantitative RT-PCR of faecal DNA (**Fig. 1B**). Demyelination was then induced by focal injection of lysolecithin into the ventral white matter of the spinal cord.

To investigate baseline differences in microglia following ABX treatment, areas of unlesioned white matter were stained with an antibody to Iba1. Microglial morphology, which correlates with activity within a given tissue (3, 22), was then analysed (**Fig. S1A**). Whilst a principal component analysis based on a number of morphological features showed clear separation between microglia from grey and white matter, there were no differences detected in microglia of unlesioned white matter following ABX treatment (**Fig. S1B, C**). This approach gave a useful indication of baseline microglial function, though we cannot exclude subtle differences that may have been resolved with more sensitive tools such as 3-dimensional morphometric analysis or RNA-sequencing (3).

The inflammatory response within lesions was examined at 7 and 14 days post lesion (dpl) by staining for CD68. Whilst CD68 is constitutively expressed at low levels in homeostatic microglia (23), we counted highly CD68-positive cells ($CD68^{hi}$)

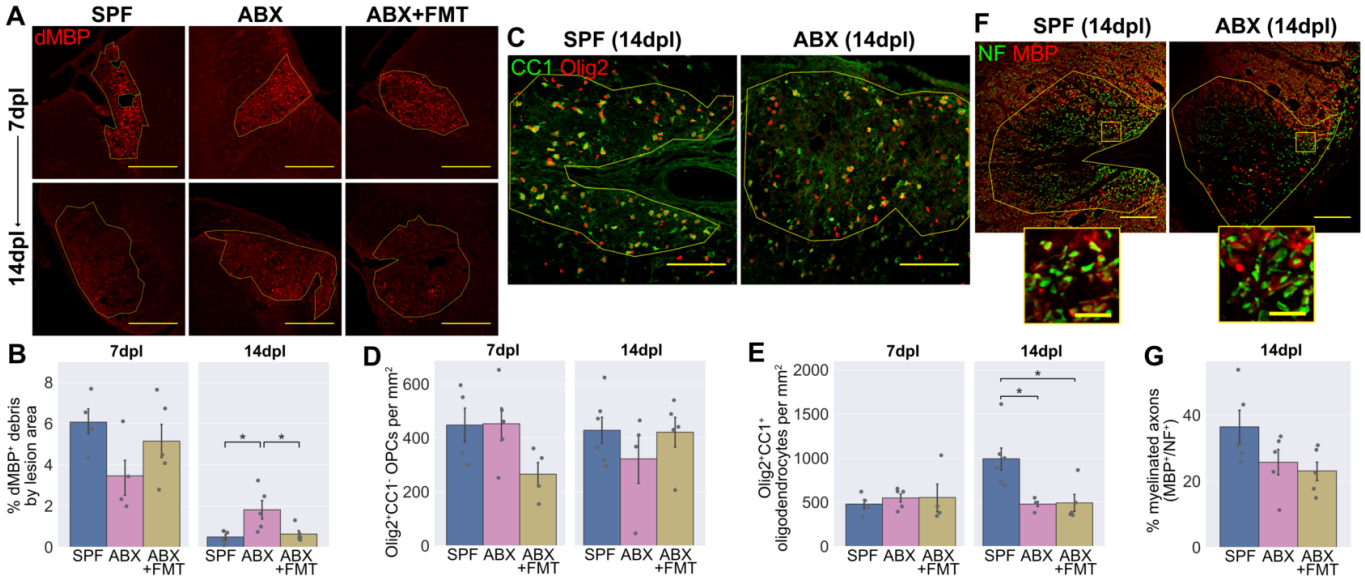

Fig. 2. Fewer new oligodendrocytes are generated in the lesions of ABX-treated mice.(**A-B**) Representative images (**A**) and area (**B**) of dMBP$^+$ myelin debris within lesions.(**C-E**) Representative images (**C**) and densities of Olig2$^+$CC1$^-$ OPCs (**D**) and Olig2$^+$CC1$^+$ oligodendrocytes (**E**) within lesions. (**F-G**) Representative images (**F**) and quantification (**G**) of NF$^+$ axons and MBP$^+$ myelin sheaths within lesions. Scale bars: (**A**) = 250μm, (**C**) = 100μm, (**F**) = 100μm [inset: 20μm]. Insets (**F**) are a 10x magnification of the boxed regions. Error bars show mean ± SEM; *p<0.05; one-way ANOVA with Tukey HSD *post hoc* test, n=4-6 mice.

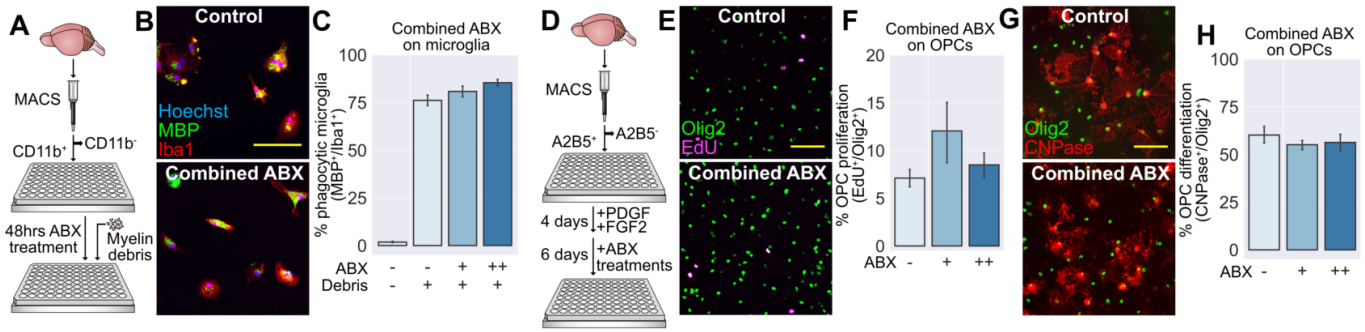

Fig. 3. Antibiotics treatment does not affect microglia phagocytosis or OPC responses *in vitro*.(**A**) Primary microglia were isolated from 3-month old mice using magnetic-activated cell sorting (MACS) for CD11b, cultured for 48 hours in the presence of antibiotics, then exposed to myelin debris for 4 hours.(**B**) Microglia were stained with an antibody to MBP to visualise myelin uptake.(**C**) Myelin uptake following exposure to combined antibiotics at their estimated CNS concentration (++) or a 10% dose (+) was comparable to control levels.(**D**) Primary OPCs were isolated from P6-8 mice using MACS for A2B5. After 4 days, antibiotics were applied, and growth factors were withdrawn to allow differentiation for 6 further days.(**E-H**) Cells were stained with an antibody to Olig2 in combination with labelling incorporated EdU to visualise proliferation (**E**) or CNPase to visualise differentiation (**G**). The antibiotic treatments had no significant effect on OPC proliferation (**F**) or differentiation (**H**).Scale bars: (**B, E, G**) = 100μm. Error bars show mean ± SEM; paired-samples *t*-test with Holm-Bonferroni correction, n=4-5 separate experiments.

– a population comprising activated microglia as well as infiltrating macrophages. At 7dpl, the density of CD68^{hi} cells was similar between ABX-treated mice and specific pathogen-free (SPF) controls (**Fig. 1C, D**), with no difference in lesion size (**Fig. S1D**). However, at 14dpl, the total density of CD68^{hi} activated microglia/macrophages was increased in lesions of mice that had received ABX treatment (**Fig. 1C, D**). To determine the reversibility of this effect, ABX-treated mice received a faecal microbial transplant (FMT) from SPF mice by oral gavage to reconstitute their microbiota. With FMT treatment, CD68^{hi} cell density remained higher than in SPF controls (**Fig. 1D**). We then asked whether the differences were driven primarily by microglia or infiltrating monocytes, by co-staining for CD68 with Tmem119, a stable marker for microglia (24). We observed that both CD68^{hi}Tmem119$^+$ microglia and CD68^{hi}Tmem119$^-$ monocyte-derived macrophages were increased in number with ABX-treatment (**Fig. 1E-G**).

Subpopulations of microglia/macrophages are known to have distinct effects in remyelination (11). We used antibodies to P2ry12 and Clec7a to identify homeostatic (P2ry12^{hi}Clec7a$^-$) and degeneration-associated (P2ry12^{lo}Clec7a$^+$) phenotypes (25, 26). At 14dpl, as well as a higher total number of CD68^{hi} cells, lesions of ABX-treated mice had fewer P2ry12^{hi}Clec7a$^-$ homeostatic microglia (**Fig. 1H, I**) and more of the P2ry12^{lo}Clec7a$^+$ degeneration-associated phenotype (**Fig. 1H, J**) than in SPF controls. We also identified a population within all lesions that expressed both high levels of P2ry12 and Clec7a (**Fig. S1O**). Staining for a panel of other microglia/macrophage markers with recognised roles in remyelination (**Fig. S1E-L**) revealed further differences between ABX-treated mice and controls. At the 7dpl timepoint, ABX-treated mice had fewer CD68^{hi} cells expressing MHC class II (MHC II, **Fig. S1E, F**) or arginase-1 (Arg1, **Fig. S1G, H**), with variable reversal following FMT.

Taken together, these results indicate that broad-spectrum antibiotic treatment results in dysregulated CNS inflammation following demyelination. Specifically, we observed an increase in total CD68^{hi} cells from 7 to 14dpl in ABX-treated groups, not seen amongst SPF controls. Coupled with this, MHC II

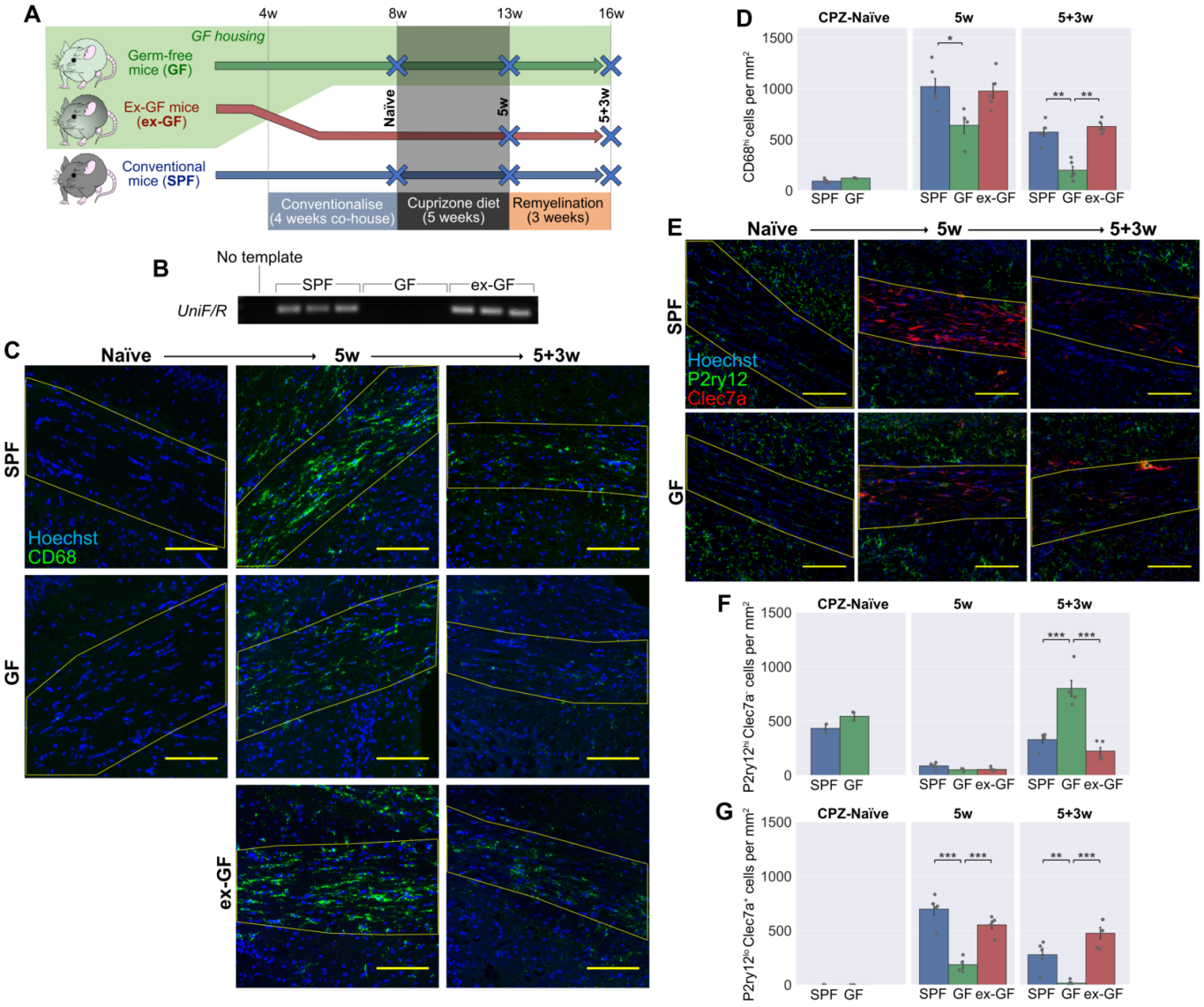

Fig. 4. Germ-free mice have an altered inflammatory response following cuprizone-mediated demyelination.(**A**) GF mice and SPF controls were fed a diet containing 0.2% cuprizone for 5 weeks from 8 weeks of age. Mice were sacrificed at the end of cuprizone administration, or after 3 weeks return to normal diet. A third group consisted of GF mice that were co-housed with SPF mice from 4 weeks of age, becoming colonised with a microbiota after weaning.(**B**) PCR for a universal prokaryotic 16S sequence in faecal DNA, demonstrating absence of this amplicon in GF mice and its presence in the ex-GF group.(**C-D**) Representative images (**C**) and density (**D**) of $CD68^{hi}$ activated microglia/macrophages within the corpus callosum (yellow line) in cuprizone-naïve mice, following 5 weeks cuprizone exposure (5w) and following a further 3 weeks of normal diet (5+3w).(**E-G**) Representative images (**E**) and density of $P2ry12^{hi}Clec7a^{-}$ homeostatic (**F**) and $P2ry12^{lo}Clec7a^{+}$ (**G**) degeneration-associated microglia/macrophages within the corpus callosum.Scale bars: (**C, E**) = 100μm. Error bars show mean ± SEM; *p<0.05, **p<0.01, ***p<0.001; one-way ANOVA with Tukey HSD *post hoc* test, n=4-5 mice.

and Arg1 expression by microglia/macrophages in the ABX-treated groups were reduced at 7dpl, and at the later timepoint there was a preponderance of the degeneration-associated microglia/macrophages with reduced numbers of $P2ry12^{hi}Clec7a^{-}$ homeostatic microglia. Thus, our microbial depletion model was dominated by a delayed but aggressive pro-inflammatory innate immune response.

Combined antibiotics treatment impairs myelin debris clearance and OPC differentiation

Central to CNS remyelination is the generation of new oligodendrocytes to restore the myelin sheath. These derive from endogenous OPCs, which migrate to lesions---, proliferate and subsequently differentiate into oligodendrocytes (5, 27). Defective differentiation from OPC to oligodendrocyte is commonly the bottleneck at which remyelination fails in human lesions and animal models (28–30). Microglia and infiltrating macrophages promote remyelination through the clearance of myelin debris, which blocks OPC differentiation in culture (31) and impairs remyelination in demyelinated lesions (12). We investigated whether the dysregulated inflammatory response following ABX treatment would be associated with reduced myelin debris clearance.

Lesions were stained with an antibody for a degraded epitope of myelin basic protein (dMBP), which becomes exposed in myelin debris (32) (**Fig. 2A, B**). At 7dpl, antibiotics did not affect the quantity of myelin debris in the lesion area. By 14dpl there had been an expected reduction in myelin debris in the SPF controls: however, this was less pronounced amongst the ABX-treated group, with more debris persisting at the later timepoint. The effect was reversed in the FMT group, which had a similar $dMBP^{+}$ area to controls.

We next explored how the OPC response would be affected by ABX treatment, using the nuclear transcription factor Olig2 to

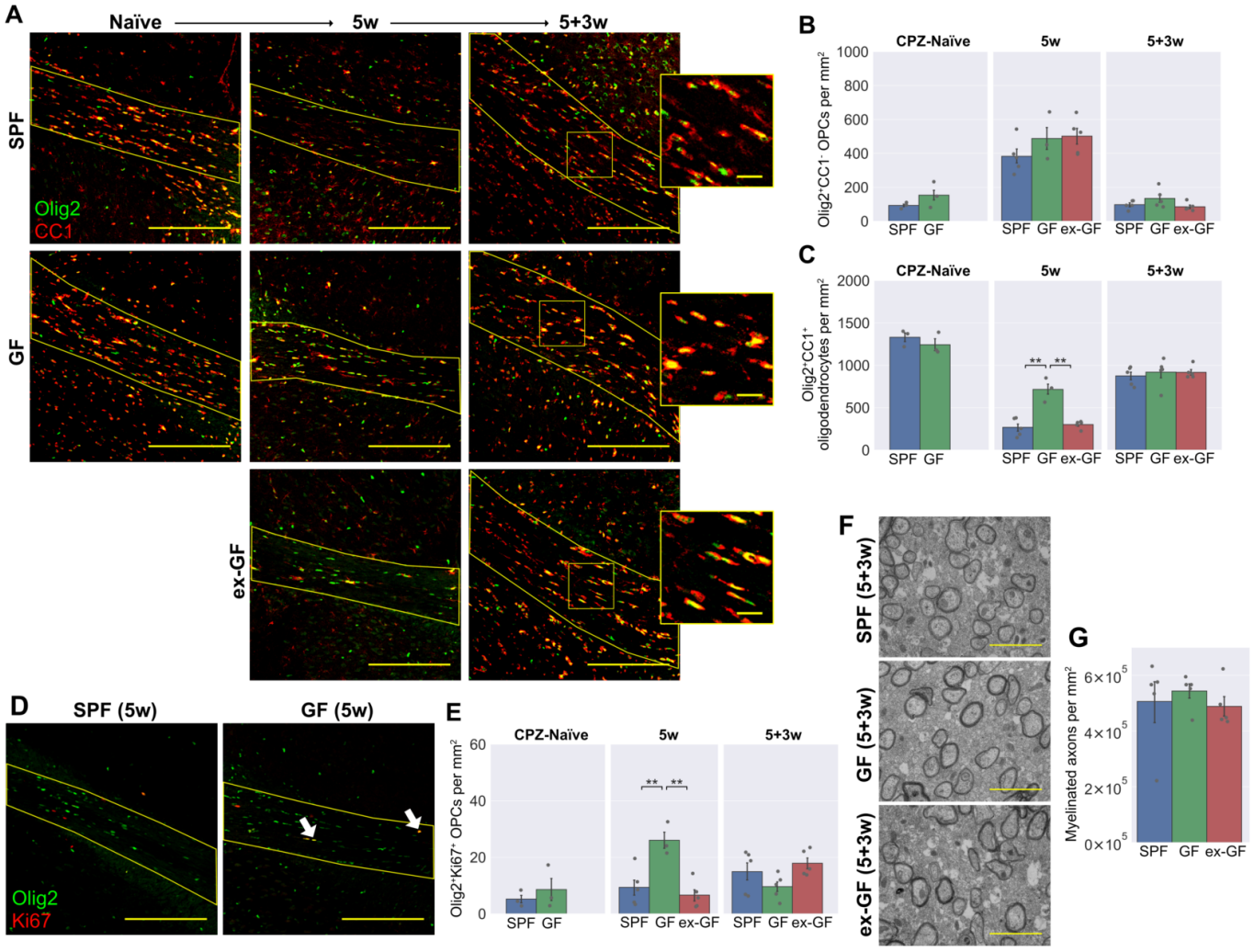

Fig. 5. Germ-free mice have reduced oligodendrocyte loss following cuprizone administration, but no difference in OPC differentiation.(**A-C**) Representative images (**A**) and density of Olig2$^+$CC1$^-$ OPCs (**B**) and Olig2$^+$CC1$^+$ mature oligodendrocytes (**C**) within the corpus callosum in cuprizone-naïve mice, following 5 weeks cuprizone exposure (5w) and following a further 3 weeks of normal diet (5+3w).(**D-E**) Representative images (**D**) and density (**E**) of Olig2$^+$Ki67$^+$ proliferating OPCs within the corpus callosum.(**F-G**) Representative electron microscopy images (**F**) and quantification (**G**) of myelinated axons within the corpus callosum 3 weeks after cuprizone cessation.Scale bars: (**A**) = 200μm [inset: 25μm], (**D**) = 200μm, (**F**) = 2μm. Insets (**A**) are a 2.5x magnification of the boxed regions. Arrow heads (**D**) show representative double-positive cells. Error bars show mean ± SEM; one-way ANOVA, n=3-5 mice.

label cells of the oligodendrocyte lineage and CC1 to distinguish differentiated oligodendrocytes (CC1$^+$) from OPCs (CC1$^-$). ABX did not affect the total number of OPCs present (**Fig. 2C, D**), nor the number of proliferating OPCs identified by Ki67 staining (**Fig. S2A, B**). However, there were fewer differentiated oligodendrocytes in the lesions of ABX-treated mice at 14dpl, suggesting a defect in OPC differentiation (**Fig. 2C, E**). This was not restored by FMT in the ABX-treated group. Finally, we quantified myelinated axons at 14dpl by counting neurofilament$^+$ axons surrounded by a ring of MBP$^+$ myelin. There were no significant differences between the groups (p=0.10, **Fig. 2F, G**).

In summary, following demyelination in ABX-treated mice, the altered inflammatory response is associated with impaired myelin debris clearance and impaired OPC differentiation. The effects of ABX treatment on remyelinating lesions could feasibly be caused by either ABX-mediated depletion of the microbiota, other off-target effects of this oral ABX regime, or a combination of these mechanisms. Two approaches were taken to explore these possibilities: 1) testing for off-target effects of ABX on relevant CNS cells in culture and 2) investigating remyelination in germ-free (GF) mice, which were reared in a sterile environment and thus were constitutionally devoid of microbes without ABX exposure.

Combined antibiotics treatment does not affect microglial phagocytosis or OPC differentiation *in vitro*

Some antibiotics are able to penetrate and act directly within the CNS. One example is the broad-spectrum tetracycline, minocycline, which can directly inhibit microglia and influence remyelination (33–35). Four of the antibiotics we administered were considered to have sufficient bioavailability to reach the CNS in significant concentrations: ampicillin, ciprofloxacin, metronidazole and the β-lactamase inhibitor sulbactam. Available pharmacokinetic data were used to estimate the concentrations these drugs would reach in the murine CNS (**Fig. S3A**), which were then applied to adult primary murine microglial cultures for 48 hours (**Fig. 3A**). Following ABX treatment, microglia were exposed to myelin debris and phagocytic uptake was quantified after 4 hours. None of the ABX individually (**Fig. S3C, D**), nor in combination (**Fig. 3B, C**), directly inhibited myelin phagocytosis by microglia. To confirm that we were not overlooking any dynamic changes by analysing a single timepoint, we also performed a timecourse of

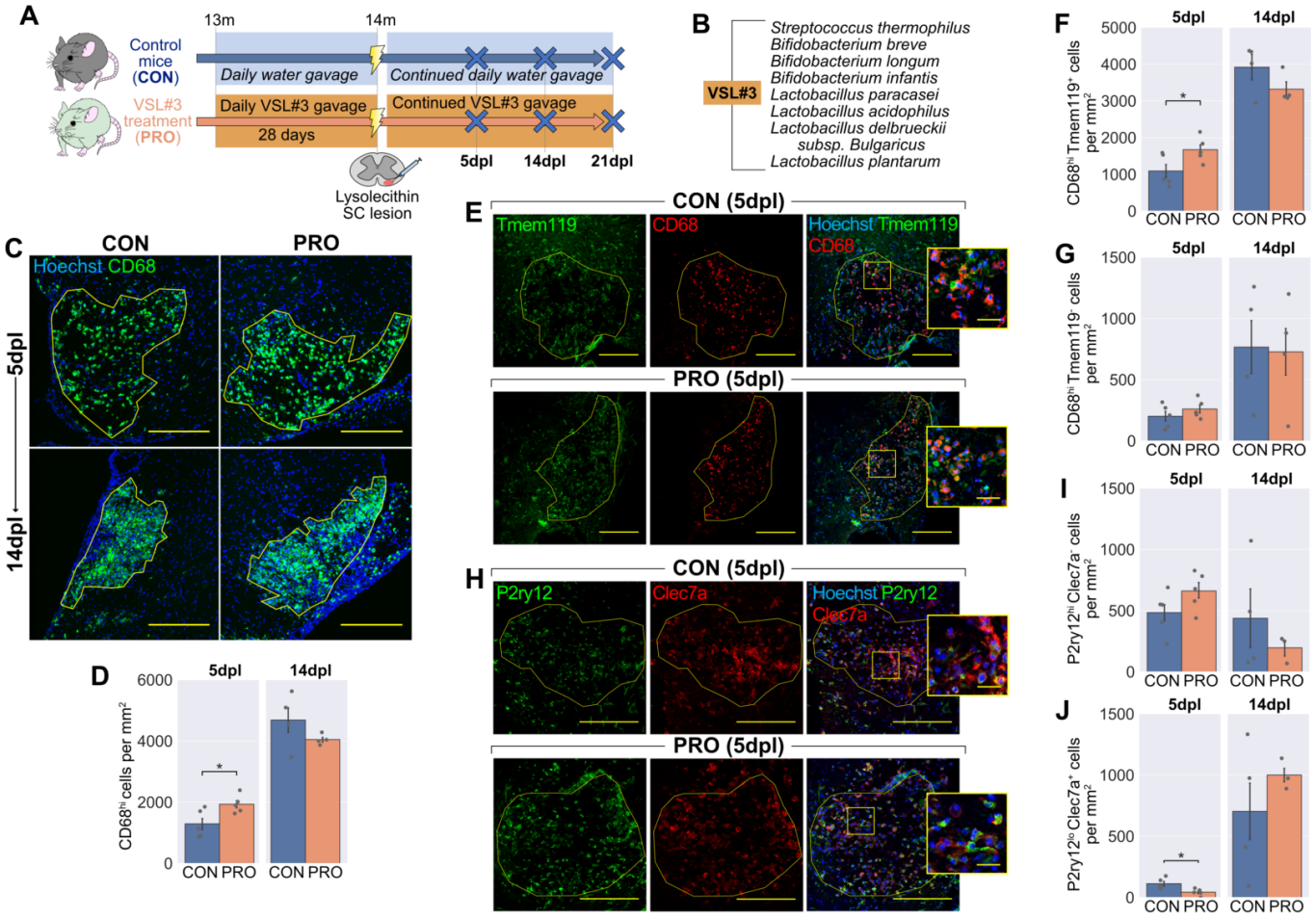

Fig. 6. Probiotic VSL#3 enhances the onset of inflammation following demyelination.(**A**) 13-month old mice were administered 1.35 x 10^9 colony-forming units (CFU) VSL#3 daily for 1 month by oral gavage. Mice were sacrificed at 5 and 14 days following lysolecithin injection into the ventral white matter of the spinal cord.(**B**) Constituent strains of VSL#3.(**C-D**) Representative images (**C**) and density (**D**) of $CD68^{hi}$ activated microglia/macrophages within lesions.(**E-G**) Representative images (**E**) and density of $Tmem119^{+}CD68^{hi}$ microglia-derived (**F**) and $Tmem119^{-}CD68^{hi}$ monocyte-derived (**G**) $CD68^{hi}$ cells within lesions.(**H-J**) Representative images (**H**) and density of $P2ry12^{hi}Clec7a^{-}$ homeostatic (**I**) of $P2ry12^{lo}Clec7a^{+}$ (**J**) degeneration-associated microglia/macrophages within lesions.Scale bars: (**C**) = 250μm, (**E, H**) = 200μm [inset: 25μm]. Insets (**E, H**) are a 3x magnification of the boxed regions. Error bars show mean ± SEM; *p<0.05; Student's *t*-test, n=3-5 mice.

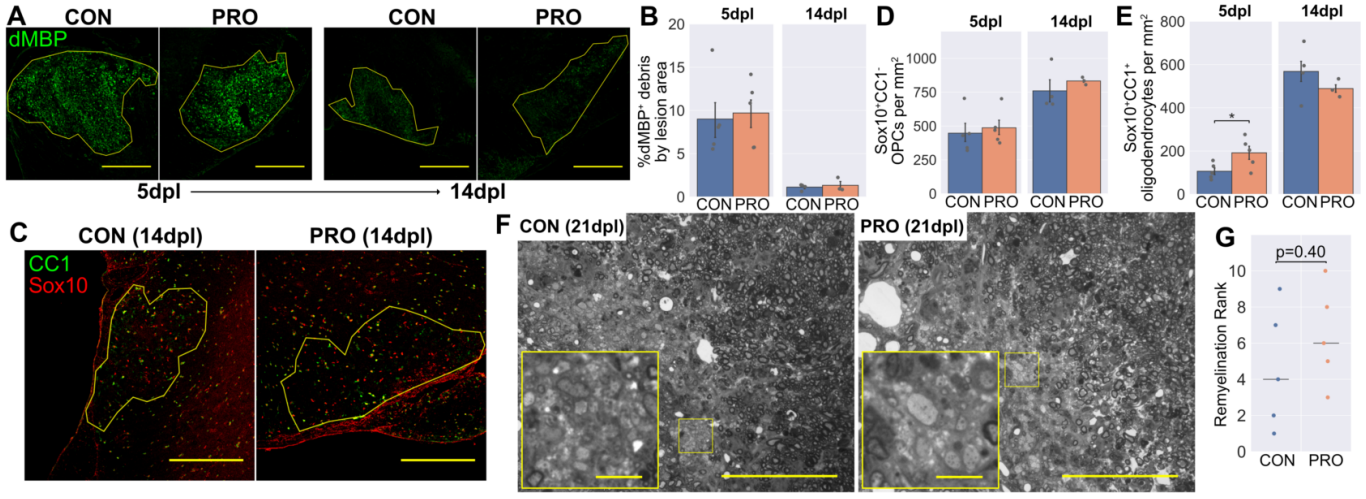

Fig. 7. VSL#3 probiotic does not enhance remyelination in aged mice. (**A-B**) Representative images (**A**) and area (**B**) of $dMBP^{+}$ myelin debris within lesions. (**C-E**) Representative images (**C**) and density of $Sox10^{+}CC1^{-}$ OPCs and (**D**) and $Sox10^{+}CC1^{+}$ mature oligodendrocytes (**E**) within lesions. (**F**) Representative images of toluidine blue-stained resin sections demonstrating persistent demyelination, typical of aged mice (CON rank: 4/10, PRO rank: 3/10). Images are shown in grayscale. (**G**) Remyelination ranks assigned by a blinded assessor, with horizontal lines showing the median for each group. Scale bars: (**A, C**) = 250μm, (**F**) = 100μm [inset: 10μm]. Insets are a 4x magnification of the boxed regions. Error bars show mean ± SEM; (**B, D, E**) Student's *t*-test, n=3-5 mice; (**G**) Mann–Whitney *U* test, n=5 mice.

phagocytosis in the presence of the combination treatment and similarly found no difference to controls conditions (**Fig. S3B**).

It is also possible that ABX can act directly on OPCs to inhibit differentiation in lesions of mice receiving oral ABX. To test this, primary cultures of murine OPCs were treated with ABX and the effects on differentiation and proliferation were determined by immunocytochemistry after six days of differentiation conditions (**Fig. 3D**). ABX treatment had no effect on OPC proliferation as measured by EdU incorporation (**Fig. 3E-F**), nor was there a difference in expression of the differentiation marker CNPase (**Fig. 3G-H**). Similarly, applying each antibiotic alone had no effect on these parameters (**Fig. S3E-H**).

Germ-free mice have an altered inflammatory response during remyelination

The results from cell culture systems suggest that the deficits observed in ABX-treated mice are not caused by direct effects of antibiotics on microglial or OPC functions critical for remyelination. However, antibiotics may have other indirect effects that are difficult to capture *in vitro*. To determine whether the microbiota can influence remyelination in the absence of ABX exposure, we investigated how remyelination would proceed in germ-free (GF) mice. As surgical lesions are impractical under the constraints of GF husbandry, we employed the cuprizone model, in which demyelination is induced by dietary administration of 0.2% cuprizone over a period of 5 weeks (**Fig. 4A**). The sterility of the GF mice was confirmed by faecal PCR for bacterial DNA (**Fig. 4B**) as well as routine in-house screening of animals and isolators using aerobic and anaerobic culture methods and microscopy of faecal smears. An ex-GF group were colonised with a microbiota after weaning, by co-housing with SPF controls, and this allowed us to distinguish developmental effects of lacking a microbiota from those reversible in adulthood. After cuprizone exposure, all mice were returned to a normal diet for a 3-week period of remyelination.

GF mice had differences in the inflammatory response that accompanied demyelination. The total number of $CD68^{hi}$ activated microglia and monocyte-derived macrophages was reduced in the GF group after the 5-week cuprizone treatment and remained so 3 weeks after cuprizone was withdrawn (**Fig. 4C, D**). To investigate this response in more detail, we quantified homeostatic ($P2ry12^{hi}Clec7a^{-}$) and degeneration-associated ($P2ry12^{lo}Clec7a^{+}$) phenotypes across the three groups (**Fig. 4E-G**). Degeneration-associated microglia/macrophages accumulated in the corpus callosum following cuprizone exposure, but this occurred to a much lesser extent in the GF group (**Fig. 4G**). In contrast, 3 weeks after cuprizone withdrawal, GF mice had higher numbers of homeostatic microglia than the other groups (**Fig. 4F**). Numbers of $CD68^{hi}$, $P2ry12^{hi}Clec7a^{-}$ and $P2ry12^{lo}Clec7a^{+}$ cells were all comparable to SPF controls in the ex-GF group, demonstrating that colonisation of GF mice can restore immune responsiveness and delineates an ongoing, dynamic role of the microbiota in the inflammatory response to tissue damage, rather than a critical window during development.

As with the ABX-treated mice, we sought to distinguish microglia and monocyte-derived macrophages. However, we observed that Tmem119 was expressed at very low levels within the corpus callosum following cuprizone exposure (**Fig. S4A**) and thus was less useful as a microglia-specific marker in this context. Instead, we quantified co-expression of Iba1 with P2ry12 (36), which remained detectable (albeit at lower levels in reactive microglia) allowing distinction between $Iba1^{+}P2ry12^{+}$ microglia and $Iba1^{+}P2ry12^{-}$ peripheral macrophages (**Fig. S4B-E**). Both microglia and monocyte-derived macrophages were reduced in GF mice after 5 weeks of cuprizone, whilst 3 weeks later the reduced CD68 expression of GF mice was primarily associated with reduced numbers of $Iba1^{+}P2ry12^{-}$ peripheral macrophages (**Fig. S4D, E**). We also stained for the same panel of microglia/macrophage markers as tested in the antibiotics experiment. Previously, ABX-treated mice were both found to have reduced expression of both MHC II and Arg1 during remyelination (**Fig. S1E-H**). Here, MHC II was similarly diminished in the remyelinating corpus callosum of GF mice, with negligible expression in microglia/macrophages of any of these animals (**Fig. S4F, G**). There was no significant reduction in Arg1, despite a similar trend (**Fig. S4H, I**), nor was there a difference detected in iNOS or MR expression in GF mice (**Fig. S4J-M**).

The deficits in the immune response of ABX-treated mice were associated with reduced myelin debris clearance after demyelination (**Fig. 2A, B**). A timecourse of cuprizone feeding in SPF mice showed that extensive $dMBP^{+}$ myelin debris after 3 weeks of cuprizone diet is subsequently cleared by 5 weeks (**Fig. S4N**). We subsequently compared dMBP staining at our 5w timepoint to determine whether myelin debris clearance was impaired under GF conditions. All groups showed similarly low levels of dMBP staining at 5w, indicating that any difference in debris clearance was not persistent beyond 5 weeks (**Fig. S4O**).

In summary, we observed that the inflammatory response following demyelination was also altered in GF mice. However, whilst lesions of ABX-treated mice were characterised by higher density of degeneration-associated microglia/macrophages, the opposite was true for cuprizone-treated GF mice, in which homeostatic microglia dominated the inflammatory response. The changes in GF mice suggest that the microbiota can indeed influence the immune response in the CNS during demyelination and remyelination; however, in this case there was no associated change in myelin debris clearance.

Germ-free mice have normal OPC differentiation during remyelination

Next, the OPC responses during cuprizone-mediated demyelination and remyelination were examined in GF mice. Prior to cuprizone exposure, GF and SPF mice had comparable numbers of $Olig2^{+}CC1^{-}$ OPCs (**Fig. 5A, B**) and $Olig2^{+}CC1^{+}$ oligodendrocytes (**Fig. 5A, C**) in the corpus callosum. Following 5 weeks cuprizone treatment, there was an 80% reduction in the density of $Olig2^{+}CC1^{+}$ oligodendrocytes in the SPF group (**Fig. 5C**). In contrast, the loss of oligodendrocytes after 5 weeks of cuprizone was less extensive amongst the GF group, whilst the ex-GF group were in line with SPF controls. At this timepoint, all groups experienced a similar rise in $Olig2^{+}CC1^{-}$ OPCs (**Fig. 5B**), consistent with the phase of OPC migration and proliferation known to occur during the first 5 weeks of cuprizone administration (45). However, when we specifically quantified $Olig2^{+}Ki67^{+}$ proliferative OPCs at 5 weeks, this was higher in the GF mice than the other two groups (**Fig. 5D, E**).

Three weeks after cuprizone withdrawal, a timepoint at which remyelination should be progressing (37, 38), all three groups exhibited a fall in OPC counts with a concurrent rise in differentiated oligodendrocytes. Importantly, there were no differences in OPC or oligodendrocyte numbers between the groups at this later timepoint (**Fig. 5B, C**), suggesting that there was no delay in OPC differentiation during the remyelination of GF mice.

Finally, the degree of remyelination following cuprizone cessation was investigated by transmission electron microscopy (**Fig. 5F**). The corpus callosum of SPF controls, GF and ex-GF mice all exhibited comparable densities of myelinated axons 3 weeks after cuprizone treatment was stopped, indicating that remyelination had progressed similarly between groups (**Fig. 5G**). The g-ratios of these axons were also measured and likewise revealed no differences (**Fig. S5A, B**).

In summary, GF mice were partially resistant to the effects of cuprizone, with less extensive oligodendrocyte loss following 5 weeks of dietary administration. This effect could be related to their diminished innate immune response during cuprizone treatment (**Fig. 4**), given that various studies have demonstrated a role

of the immune system, particularly microglia and neutrophils, in mediating cuprizone-induced demyelination (39, 40). The late peak in OPC proliferation observed in the GF group (**Fig. 5D, E**), may similarly be in response to a sluggish innate immune response. However, 3 weeks after cuprizone was stopped, the absence of any difference in OPC or oligodendrocyte numbers combined with similar densities of myelinated axons suggest that remyelination itself is unaffected in GF mice.

Probiotic VSL#3 can augment the innate immune response during CNS remyelination

Taking the results from the antibiotics and germ-free experiments, together with *in vitro* studies, an intact microbiota appears to be necessary for the appropriate inflammatory response during remyelination. However, the effect that microbial depletion has on OPC responses, and thus remyelination itself, remains less certain. We next explored the inverse of this relationship: whether the microbiota can be manipulated therapeutically to enhance appropriate inflammatory responses and subsequently remyelination. For this, we used older mice (aged 14 months) in which remyelination occurs more slowly with scope for improvement (14, 41). These mice were administered the probiotic VSL#3 by daily gavage for 1 month, prior to inducing focal demyelination in the spinal cord white matter by lysolecithin injection (**Fig. 6A**).

VSL#3, a freeze-dried formulation of 8 strains of Gram-positive bacteria (**Fig. 6B**), was chosen due to its good survival on transit through the GI tract (42) and several characterised therapeutic effects in the CNS (4, 43, 44). Additionally, VSL#3 enhanced concentrations of short chains fatty acids (SCFAs) in the faeces and serum of mice (**Fig. S6B, D**), consistent with a previous study (45). The SCFAs acetate, butyrate and propionate are microbial metabolites that are depleted in GF mice (**Fig. S5A, C**) and considered key signalling molecules in how the microbiota influence CNS inflammation (3, 46).

Following VSL#3 treatment, there was a mild enhancement in the inflammatory response at 5dpl, with greater density of $CD68^{hi}$ activated microglia and infiltrating macrophages (**Fig. 6C, D**). We again stained for CD68 in combination with Tmem119 to determine which populations of $CD68^{hi}$ cells were affected. We found that probiotic administration increased numbers of $CD68^{hi}Tmem119^{+}$ microglia at 5dpl (**Fig. 6E, F**), though no difference was detected amongst $CD68^{hi}Tmem119^{-}$ monocyte-derived macrophages (**Fig. 6E, G**). Staining for P2ry12 and Clec7a revealed that, despite the increase in total number of $CD68^{hi}$ cells at 5dpl, the numbers of $P2ry12^{lo}Clec7a^{+}$ degeneration-associated microglia/macrophages were reduced with VSL#3 (**Fig. 6H-J**), suggesting a less detrimental inflammatory environment. Both iNOS and MR were expressed by greater numbers of $CD68^{hi}$ cells in lesions following probiotic treatment at 5dpl (**Fig. S6E-H**), whilst two markers initially reduced by ABX (MHC II and Arg1) were not significantly enhanced by probiotic treatment (**Fig. S6I-L**).

No differences were detected at 14dpl, a timepoint at which debris should be largely cleared and newly differentiated oligodendrocytes initiate remyelination. Thus, although our probiotic augmented the initial inflammatory response at 5dpl, the effect of this on subsequent trajectory of inflammation in the lesion was more limited.

VSL#3 does not improve the outcome of remyelination

Finally, we assessed whether this inflammatory enhancement during the early stages would contribute to a better outcome in remyelination. In contrast to ABX-treated mice, in which the altered inflammatory response resulted in prolonged presence of myelin debris, myelin debris was not cleared any faster in the lesions of probiotic-treated mice (**Fig. 7A, B**). Consistent with this, there was no difference in the OPC response, with OPC number (**Fig. 7C, D; Fig. S7A**), proliferation (**Fig. S7B, C**) and differentiation of new oligodendrocytes at 14dpl (**Fig. 7C, E**) unchanged by probiotic treatment. There was a small increase in the number of oligodendrocytes present at 5dpl (**Fig. 7E; Fig. S7A**). As this timepoint is considered too early for significant OPC differentiation to occur, even in young adults (47) and taking into account that no difference was observed at 14dpl, the peak time for OPC differentiation, this likely reflects a reduction in oligodendrocyte death, rather than enhanced OPC differentiation.

To confirm that there was no therapeutic effect of VSL#3 on remyelination, semi-thin resin sections were taken at a later timepoint (21dpl) and myelin stained with toluidine-blue (**Fig. 7F**). The completion of remyelination was ranked by two blinded assessors, neither of whom detected a difference in remyelination between groups (**Fig. 7G**).

Thus, administration of the probiotic VSL#3 promoted a stronger initial inflammatory response in aged mice following demyelination. However, this did not lead to faster clearance of myelin debris or OPC differentiation, and overall remyelination was unchanged compared to control mice.

Discussion

The aim of these experiments was to explore how the microbiota can influence remyelination in the mammalian CNS. Across all three models, the responses of microglia and infiltrating macrophages were modulated by interventions that altered the microbiota. Broadly, this amounted to a dysregulated immune response in ABX-treated mice, and a blunted, more homeostatic-type response in GF mice. In contrast, VSL#3 probiotic treatment enhanced the onset of inflammation whilst reducing numbers of damage-associated microglia/macrophages. As remyelination depends upon a coordinated immune response (9–11, 48), such changes might be expected to impact upon the OPC activity underlying remyelination. Consistent with this hypothesis, ABX-treated mice had deficits in myelin debris clearance and OPC differentiation. However, these findings were neither replicated in GF mice, nor reversed by probiotic administration. Bringing together these findings from different models, the microbiota appears to shape the inflammatory response during CNS remyelination, but the effect of this on regenerative responses by OPCs is limited.

We can postulate what the reasons may be for this disparity, in which modulating the microbiota alters CNS inflammatory responses without simultaneous changes in the efficiency of remyelination itself. It could be that the inflammatory changes that our interventions provoked via the microbiota were simply not sufficient to alter remyelination. This may be either a quantitative limit (i.e. the changes in CNS inflammation caused by microbiota modulation were too subtle), or a more qualitative limit (i.e. the specific functions of microglia/macrophages that were affected had minimal effect on remyelination). Indeed, as new molecular techniques reveal further insights into microglial/macrophage heterogeneity, the specific roles of these different phenotypes during remyelination remain to be fully elucidated (25, 26). Similarly, it cannot be excluded that other microbiota-based interventions might be more fruitful in producing changes in the efficiency of remyelination. However, we believe that our negative result showing a lack of impact on remyelination using GF mice is evidence against such a powerful influence.

In vitro, ABX did not directly influence microglial phagocytosis or OPC differentiation, though other indirect effects of ABX are difficult to exclude. Indeed, the differing balance of homeostatic and damage-associated microglia/macrophages between GF and ABX-treated mice imply that our ABX treatment did not simply imitate GF conditions. This may be due to other "off-target" effects (undetected in our cell culture studies), or perhaps an incomplete depletion of the microbiota, in turn allowing other microorganisms to thrive. Notably, whilst our ABX regime re-

duced bacterial DNA by approximately 100-fold, other studies have achieved a more extensive depletion (4). Regardless, the lack of an effect on the proportion of myelinated axons at 14dpl is evidence that remyelination itself is resilient to the changes in inflammation that we provoked using antibiotics.

Interactions between microbiota and regeneration have been observed in other tissues where contact is more direct. Skin wounds heal faster in GF mice, associated with reduced neutrophil accumulation (49), whilst microbiota-derived lipopolysaccharide (LPS) was found to dictate regenerative responses in the intestinal crypt (50). Similarly, the regenerative capacity of planaria was diminished by pathogenic shifts in their microbiota (51). However, it seems likely that such interactions become less relevant at anatomically distant sites – for example, the evidence linking liver regeneration to the microbiota is more contentious (52, 53). Outside a regenerative context, changes in developmental or adaptive myelination in the CNS have previously been linked to the microbiota. GF mice are hypermyelinated specifically in the prefrontal cortex (PFC) (54), whilst a PFC *hypo*myelination phenotype could be transferred between different strains of mice by FMT (55). Whilst a role for the microbiota in myelin homeostasis is exciting, the findings of both studies were region-specific and occur in a very different context to remyelination, which is accompanied by tissue damage and a robust inflammatory response.

Though neither our GF nor probiotic study demonstrated a difference in remyelination, in both cases there was a protective effect of the intervention on demyelination, as seen by increased numbers of oligodendrocytes at timepoints too early for substantial OPC differentiation to have occurred. This could be explained by the role of the immune system in mediating demyelination as well as remyelination in the lysolecithin and cuprizone models (47, 48, 56, 57). Consistent with this idea, we observed that both of these manipulations of the microbiota were associated with reduced numbers of P2ry12^{lo}Clec7a^{+} degeneration-associated microglia/macrophages within the lesion. Similarly, GF mice were resistant to immune-mediated CNS pathology in a model of Parkinson's disease (46), whilst changes in the immune response with VSL#3 treatment were associated with white matter preservation in a spinal cord contusion model (44). As the immune system plays a prominent role in demyelination in MS, the majority of previous work on the gut-brain axis has focused on interventions that can limit inflammation and demyelination. For example, in the immune-driven experimental autoimmune encephalomyelitis (EAE) model, GF or antibiotics-treated mice are resistant to demyelination (19, 58, 59).

In conclusion, we have highlighted the microbiota as a contributing factor to the inflammatory response during CNS remyelination. However, the regenerative responses of OPCs were largely independent of our interventions. The exception to this was following broad-spectrum oral antibiotic treatment, during which antibiotics do not inhibit OPCs directly, but may have other off-target systemic effects. These findings identify high, combined doses of oral antibiotics as a negative influence on OPC responses during remyelination and further our understanding of the interaction between the microbiota and mammalian regeneration.

Materials and methods

For full details, see **SI Appendix, Supplementary Materials and Methods**.

Animal work. All animal work complied with the requirements and regulations of the United Kingdom Home Office (Project Licences: 70/7715 and 2789) or the European Guidelines for animal welfare with approval from the "Landesamt für Gesundheit und Soziales" (LAGeSo, Berlin registration number: G0184/12).

Focal lysolecithin lesions in antibiotics-treated mice. A cocktail of antibiotics was administered via the drinking water to 4-month old female C57BL/6 mice for 8 weeks. The antibiotics used were: ampicillin/sulbactam (1.5g/L), ciprofloxacin (200mg/L), vancomycin (500mg/L), metronidazole (1g/L) and imipenem (250mg/L) – a regime previously employed to cause depletion of microbes in the gut (4, 60). The faecal transplant group were then orally gavaged with faecal material from control mice, once per day for 5 days, whilst the antibiotics group continued to receive the antibiotics for the duration of the experiment. The control group were housed in specific pathogen free (SPF) conditions throughout. At age 7 months, demyelination was initiated by stereotactic injection of 1µl lysolecithin (L4129, Sigma-Aldrich, UK) into the thoracic spinal cord ventral white matter.

Cuprizone administration to germ-free mice. Male C57BL/6 mice were bred from a GF nucleus colony at the University of East Anglia and maintained in a flexible-film isolator, supplied with sterilised air, food, water and bedding. The GF group were maintained in these conditions throughout the experiment and compared to aged-matched SPF controls. The ex-GF mice were littermates of the GF group and remained in GF conditions until after weaning (4 weeks old), at which point they acquired a microbiome by co-housing with the SPF mice. Demyelination was initiated by administration of a 0.2% cuprizone diet (TD.140803, Envigo, Huntingdon, UK), which received 50kGy γ-irradiation for sterilisation. All groups received the cuprizone diet for 5 weeks beginning at age 2 months in place of their regular diet and were then returned to regular diet for 3 weeks afterwards.

Focal lysolecithin lesions in probiotic-treated mice. 13-month old female C57BL/6 mice were administered a daily dose of $1.35x10^9$ colony forming units of VSL#3 (a gift from Janine DeBeer, Ferring Pharmaceuticals, London, UK), suspended in 100µl autoclaved water by oral gavage for 28 days. These were compared to age-matched control mice, which were instead gavaged daily with 100µl water. All groups received a focal injection of lysolecithin as described in the antibiotics study.

Histological analysis. Standard techniques for immunohistochemistry and preparation of resin sections were applied, as described previously (61). For a full list of antibodies, please see **SI appendix, Supplementary Materials and Methods**.

Cell culture. Microglia were isolated from 3-month old adult C57BL/6 mice using a Magnetic-Activated Cell Sorting (MACS) protocol (**Fig. 3A**), similar to that described previously (62). After 48 hours, media was changed to macrophage serum-free medium (Thermo Fisher Scientific, San Diego, CA), containing the antibiotic treatments (**Fig. S2A**). Following a further 48 hours, 10µg/ml myelin debris was added to each well for 4 hours.

OPCs were isolated from P6-8 C57BL/6 mouse pups using a MACS protocol (**Fig. 3D**), similar to that described previously (62). Cultures received growth factors for the first 4 days (PDGFα and FGF2), after which antibiotic treatments (**Fig. S2A**) were introduced for a further six days (replaced after 3 days) in the absence of growth factors to allow differentiation. 10µM 5-ethynyl-2'-deoxyuridine (EdU) was applied for 3 hours prior to fixation.

Standard immunocytochemistry techniques were applied, as described previously (62). For a full list of antibodies, please see **SI appendix, Supplementary Materials and Methods**.

Image analysis. Cell counts were semi-automated, using a combination of *Fiji*, *CellProfiler* and *CellProfiler Analyst* software (63). The region of interest (ROI i.e. the lesion area) was manually defined by a blinded observer using a composite image, based on Hoechst^{+} hypercellularity and non-specific background staining. To quantify the area of a lesion occupied by myelin debris, a threshold determined by background (median) dMBP staining was applied to images in *CellProfiler*.

To quantify remyelination from toluidine blue-stained resin sections in the probiotic study, slides of the 10 lesions (5 per group) were independently ranked by two experienced, blinded investigators (GG and CZ) according to the extent of remyelination. Ranks were based upon the proportion of each lesion with thin myelin sheaths characteristic of remyelination, compared to areas with persistently demyelinated axons. The assigned numerical order (1-10) was used for subsequent non-parametric statistical tests. To quantify remyelination from electron microscopy images, the internal and external diameter of myelin sheaths were traced using a freehand selection tool in *Fiji*. The g-ratio was calculated as the ratio between the diameters of two circles with areas equal to the internal and external selections respectively.

Statistical analysis. All statistical analysis was carried out using a *Jupyter* Notebook with *Python 2*. *In vivo* experiments contained the following numbers of biological replicates per group: antibiotics lysolecithin study: n=4-6 mice, germ-free cuprizone study: n=4-5 mice, probiotic lysolecithin study: n=3-5 mice. These group sizes were chosen based on previous work and were thought to be sufficiently powered to detect meaningful differences in the OPC / inflammatory response to demyelination. For *in vivo* cell counts, generally 3-4 technical replicate sections were counted and averaged per biological replicate. For *in vitro* cell assays, 3-5 technical replicate wells were averaged for each of 4-5 biological replicate studies.

Data was tested for normality of residuals (Kolmogorov-Smirnov test) and homogeneity of variance (Levene's test). Data sets passing both of these criteria were compared by either unpaired Student's t-test (if 2 groups), or one-way ANOVA with Tukey HSD *post hoc* tests (if >2 groups). Non-parametric data was compared by Mann-Whitney U test (2 groups) or Kruskal-Wallis test with Dunn's *post hoc* test (>2 groups). For *in vitro* assays, treated conditions were compared to control conditions using a paired-samples t-test with the Holm-Bonferroni correction for multiple comparisons. For all statistical tests, differences were considered significant if $p<0.05$, and the respective test is described in each figure legend.

In all bar plots, the height of the bar represents the group mean, with an error bar representing the standard error of the mean (SEM). *In vivo* data

are overlaid with strip plots, in which a grey point represents the value for each individual animal.

Acknowledgements

We thank Andrew Goldson and Arlaine Brion (Quadram Institute) for their expertise and assistance in running the GF study. We are also grateful to Daniel Morrison and Michal Presz for their technical assistance and to the Cambridge Advanced Imaging Centre for use of their electron microscope.

This work was supported by grants from UK Multiple Sclerosis Society, The British Trust for the Myelin Project, MedImmune, The Adelson Medical Research Foundation, Wellcome Trust, BBSRC, the Leverhulme Trust and a core support grant from the Wellcome Trust and MRC to the Wellcome Trust - Medical Research Council Cambridge Stem Cell Institute. CEM was supported by grants from the Jean Shanks Foundation and the James Baird Fund, AGF was supported by an ECTRIMS fellowship and OBZ received a BIRAX fellowship.

1. T. C. Fung, C. A. Olson, E. Y. Hsiao, Interactions between the microbiota, immune and nervous systems in health and disease. *Nat. Neurosci.* **20**, 145–155 (2017).
2. A. B. Aurora, E. N. Olson, Immune modulation of stem cells and regeneration. *Cell Stem Cell* **15**, 14–25 (2014).
3. D. Erny et al., Host microbiota constantly control maturation and function of microglia in the CNS. *Nat. Neurosci.* **18**, 965–977 (2015).
4. L. Möhle et al., Ly6Chi Monocytes provide a link between antibiotic-induced changes in gut microbiota and adult hippocampal neurogenesis. *Cell Rep.* **15**, 1945–1956 (2016).
5. R. J. M. Franklin, C. Ffrench-Constant, Regenerating CNS myelin — from mechanisms to experimental medicines. *Nat. Rev. Neurosci.* **18**, 753–769 (2017).
6. K. J. Smith, W. F. Blakemore, W. I. McDonald, Central remyelination restores secure conduction. *Nature* **280**, 395–396 (1979).
7. I. D. Duncan et al., Extensive remyelination of the CNS leads to functional recovery. *Proc. Natl. Acad. Sci.* **106**, 6832–6836 (2009).
8. K. A. Irvine, W. F. Blakemore, Remyelination protects axons from demyelination-associated axon degeneration. *Brain* **131**, 1464–1477 (2008).
9. M. R. Kotter et al., Macrophage depletion impairs oligodendrocyte remyelination following lysolecithin-induced demyelination. *Glia* **35**, 204–12 (2001).
10. C. Zhao, W.-W. Li, R. J. M. Franklin, Differences in the early inflammatory responses to toxin-induced demyelination are associated with the age-related decline in CNS remyelination. *Neurobiol. Aging* **27**, 1298–307 (2006).
11. V. E. Miron et al., M2 microglia and macrophages drive oligodendrocyte differentiation during CNS remyelination. *Nat. Neurosci.* **16**, 1211–1218 (2013).
12. M. R. Kotter, W.-W. Li, C. Zhao, R. J. M. Franklin, Myelin impairs CNS remyelination by inhibiting oligodendrocyte precursor cell differentiation. *J. Neurosci.* **26**, 328–32 (2006).
13. T. J. Yuen et al., Identification of endothelin 2 as an inflammatory factor that promotes central nervous system remyelination. *Brain* **136**, 1035–1047 (2013).
14. J. M. Ruckh et al., Rejuvenation of regeneration in the aging central nervous system. *Cell Stem Cell* **10**, 96–103 (2012).
15. M. S. Natrajan et al., Retinoid X receptor activation reverses age-related deficiencies in myelin debris phagocytosis and remyelination. *Brain* **138**, 3581–3597 (2015).
16. J. Chen et al., Multiple sclerosis patients have a distinct gut microbiota compared to healthy controls. *Sci Rep* **6**, 28484 (2016).
17. S. Jangi et al., Alterations of the human gut microbiome in multiple sclerosis. *Nat. Commun.* **7**, 12015 (2016).
18. K. Berer et al., Gut microbiota from multiple sclerosis patients enables spontaneous autoimmune encephalomyelitis in mice. *Proc. Natl. Acad. Sci.* **114**, 10719–10724 (2017).
19. J. Ochoa-Reparaz et al., Role of gut commensal microflora in the development of experimental autoimmune encephalomyelitis. *J. Immunol.* **183**, 6041–6050 (2009).
20. S. Tankou et al., Treatment of EAE and MS subjects with probiotic VSL#3 (P5.320). *Neurology* **86** (2016).
21. E. Kouchaki et al., Clinical and metabolic response to probiotic supplementation in patients with multiple sclerosis: A randomized, double-blind, placebo-controlled trial. *Clin. Nutr.* **36**, 1245–1249 (2017).
22. B. M. Davis et al., Characterizing microglia activation: a spatial statistics approach to maximize information extraction. *Sci. Rep.* **7**, 1576 (2017).
23. V. H. Perry, J. Teeling, Microglia and macrophages of the central nervous system: The contribution of microglia priming and systemic inflammation to chronic neurodegeneration. *Semin. Immunopathol.* **35**, 601–612 (2013).
24. M. L. Bennett et al., New tools for studying microglia in the mouse and human CNS. *Proc. Natl. Acad. Sci.* **113**, E1738–E1746 (2016).
25. S. Krasemann et al., The TREM2-APOE pathway drives the transcriptional phenotype of dysfunctional microglia in neurodegenerative diseases. *Immunity* **47**, 566-581.e9 (2017).
26. H. Keren-Shaul et al., A unique microglia type associated with restricting development of Alzheimer's disease. *Cell* **169**, 1276-1290.e17 (2017).
27. M. Zawadzka et al., CNS-resident glial progenitor/stem cells produce Schwann cells as well as oligodendrocytes during repair of CNS demyelination. *Cell Stem Cell* **6**, 578–90 (2010).
28. R. H. Woodruff, M. Fruttiger, W. D. Richardson, R. J. M. Franklin, Platelet-derived growth factor regulates oligodendrocyte progenitor numbers in adult CNS and their response following CNS demyelination. *Mol. Cell. Neurosci.* **25**, 252–262 (2004).
29. A. Chang et al., NG2-positive oligodendrocyte progenitor cells in adult human brain and multiple sclerosis lesions. *J. Neurosci.* **20**, 6404–12 (2000).
30. G. Wolswijk, Chronic stage multiple sclerosis lesions contain a relatively quiescent population of oligodendrocyte precursor cells. *J. Neurosci.* **18**, 601–9 (1998).
31. S. Robinson, R. H. Miller, Contact with central nervous system myelin inhibits oligodendrocyte progenitor maturation. *Dev. Biol.* **216**, 359–368 (1999).
32. A. Matsuo et al., Unmasking of an unusual myelin basic protein epitope during the process of myelin degeneration in humans: a potential mechanism for the generation of autoantigens. *Am. J. Pathol.* **150**, 1253–66 (1997).
33. M. Nikodemova et al., Minocycline down-regulates MHC II expression in microglia and macrophages through inhibition of IRF-1 and Protein Kinase C (PKC) α/βII. *J. Biol. Chem.* **282**, 15208–15216 (2007).
34. A. Defaux, M.-G. Zurich, P. Honegger, F. Monnet-Tschudi, Minocycline promotes remyelination in aggregating rat brain cell cultures after interferon-γ plus lipopolysaccharide-induced demyelination. *Neuroscience* **187**, 84–92 (2011).
35. T. Tanaka, K. Murakami, Y. Bando, S. Yoshida, Minocycline reduces remyelination by suppressing ciliary neurotrophic factor expression after cuprizone-induced demyelination. *J. Neurochem.* **127**, 259–70 (2013).
36. O. Butovsky et al., Identification of a unique TGF-β–dependent molecular and functional signature in microglia. *Nat. Neurosci.* **17**, 131–143 (2014).
37. J. Praet et al., Cellular and molecular neuropathology of the cuprizone mouse model: Clinical relevance for multiple sclerosis. *Neurosci. Biobehav. Rev.* **47**, 485–505 (2014).
38. A. J. Steelman, J. P. Thompson, J. Li, Demyelination and remyelination in anatomically distinct regions of the corpus callosum following cuprizone intoxication. *Neurosci. Res.* **72**, 32–42 (2012).
39. T. Clarner et al., CXCL10 triggers early microglial activation in the cuprizone model. *J. Immunol.* **194**, 3400–3413 (2015).
40. L. Liu et al., CXCR2-positive neutrophils are essential for cuprizone-induced demyelination: relevance to multiple sclerosis. *Nat. Neurosci.* **13**, 319–326 (2010).
41. J. K. Huang et al., Retinoid X receptor gamma signaling accelerates CNS remyelination. *Nat. Neurosci.* **14**, 45–53 (2011).
42. M. Fredua-Agyeman, S. Gaisford, Comparative survival of commercial probiotic formulations: Tests in biorelevant gastric fluids and real-time measurements using microcalorimetry. *Benef. Microbes* **6**, 141–151 (2015).
43. E. Distrutti et al., Modulation of intestinal microbiota by the probiotic VSL#3 resets brain gene expression and ameliorates the age-related deficit in LTP. *PLoS One* **9**, (2014).
44. K. A. Kigerl et al., Gut dysbiosis impairs recovery after spinal cord injury. *J. Exp. Med.* **213**, 2603–2620 (2016).
45. H. Yadav et al., Beneficial metabolic effects of a probiotic via butyrate-induced GLP-1 hormone secretion. *J. Biol. Chem.* **288**, 25088–25097 (2013).
46. T. R. Sampson et al., Gut microbiota regulate motor deficits and neuroinflammation in a model of Parkinson's disease. *Cell* **167**, 1469-1480.e12 (2016).
47. M. B. Keough, S. K. Jensen, V. W. Yong, Experimental demyelination and remyelination of murine spinal cord by focal injection of lysolecithin. *J. Vis. Exp.* e52679 (2015).
48. A. F. Lloyd et al., Central nervous system regeneration is driven by microglia necroptosis and repopulation. *Nat. Neurosci.* **22**, (2019).
49. M. C. C. Canesso et al., Skin wound healing is accelerated and scarless in the absence of commensal microbiota. *J. Immunol.* **193**, 5171–5180 (2014).
50. T. Naito et al., Lipopolysaccharide from crypt-specific core microbiota modulates the colonic epithelial proliferation-to-differentiation balance. *MBio* **8**, 1–16 (2017).
51. C. P. Arnold et al., Pathogenic shifts in endogenous microbiota impede tissue regeneration via distinct activation of TAK1/MKK/p38. *Elife* **5**, e16793 (2016).
52. R. P. Cornell, B. L. Liljequist, K. F. Bartizal, Depressed liver regeneration after partial hepatectomy of germ-free, athymic and lipopolysaccharide-resistant mice. *Hepatology* **11**, 916–922 (1990).
53. T. Malinka et al., P0002 : Liver regeneration is not impacted in the absence of intestinal microbiota. *J. Hepatol.* **62**, S291 (2015).
54. A. E. Hoban et al., Regulation of prefrontal cortex myelination by the microbiota. *Transl. Psychiatry* **6**, e774 (2016).
55. M. Gacias et al., Microbiota-driven transcriptional changes in prefrontal cortex override genetic differences in social behavior. *Elife* **5**, e13442 (2016).
56. S. S. Ousman, S. David, Lysophosphatidylcholine induces rapid recruitment and activation of macrophages in the adult mouse spinal cord. *Glia* **30**, 92–104 (2000).
57. N. Ghasemlou, S. Y. Jeong, S. Lacroix, S. David, T cells contribute to lysophosphatidylcholine-induced macrophage activation and demyelination in the CNS. *Glia* **55**, 294–302 (2007).
58. K. Berer et al., Commensal microbiota and myelin autoantigen cooperate to trigger autoimmune demyelination. *Nature* **479**, 538–41 (2011).
59. Y. K. Lee, J. S. Menezes, Y. Umesaki, S. K. Mazmanian, Proinflammatory T-cell responses to gut microbiota promote experimental autoimmune encephalomyelitis. *Proc. Natl. Acad. Sci.* **108**, 4615–4622 (2011).
60. M. M. Heimesaat et al., Gram-negative bacteria aggravate murine small intestinal Th1-type immunopathology following oral infection with Toxoplasma gondii. *J. Immunol.* **177**, 8785–8795 (2006).
61. De La Fuente AG et al., Pericytes stimulate oligodendrocyte progenitor cell differentiation during CNS remyelination. *Cell Rep.* **20**, 1755-1764 (2017).
62. R. Baror et al., Transforming growth factor-beta renders ageing microglia inhibitory to oligodendrocyte generation by CNS progenitors. *Glia* **67**, 1374-1384 (2019).
63. A. E. Carpenter et al., CellProfiler: image analysis software for identifying and quantifying cell phenotypes. *Genome Biol.* **7**, R100 (2006).

Please review all the figures in this paginated PDF and check if the figure size is appropriate to allow reading of the text in the figure.

If readability needs to be improved then resize the figure again in 'Figure sizing' interface of Article Sizing Tool.